Electronic Supplementary Material (ESI) for Nanoscale.
This journal is © The Royal Society of Chemistry 2019

Supporting Information

Stabilization of a monolayer tellurene phase at CdTe interfaces

Tadas Paulauskas,* Fatih G. Sen, Ce Sun, Paolo Longo, Yuan Zhang, Saw Wai Hla,

Moon J. Kim, Maria K.Y. Chan, and Robert F. Klie

Supporting information contents:

1. {100}B CdTe bicrystal interface
2. Energy dispersive X-ray spectroscopy raw data of tellurene
3. *GW* and PBE band structure of tellurene without spin-orbit coupling
4. Simulated EELS from *GW* calculations

1. {001}B CdTe bicrystal interface

Figure S1 shows cross-sectional atomic-resolution HAADF and EDX images of the {001}B interface along the CdTe <110> zone-axis. CdTe wafers, in this case, are bonded with Te-terminated {001} planes facing each other. The interface chemistry is verified in Figure S1 (b). These images present one common type of atomic-ordering observed in this bicrystal whereby an additional set of Te atomic-columns appear next to the CdTe dumbbells at the interface. The wafers are also clearly shifted along the vertical with respect to one another.

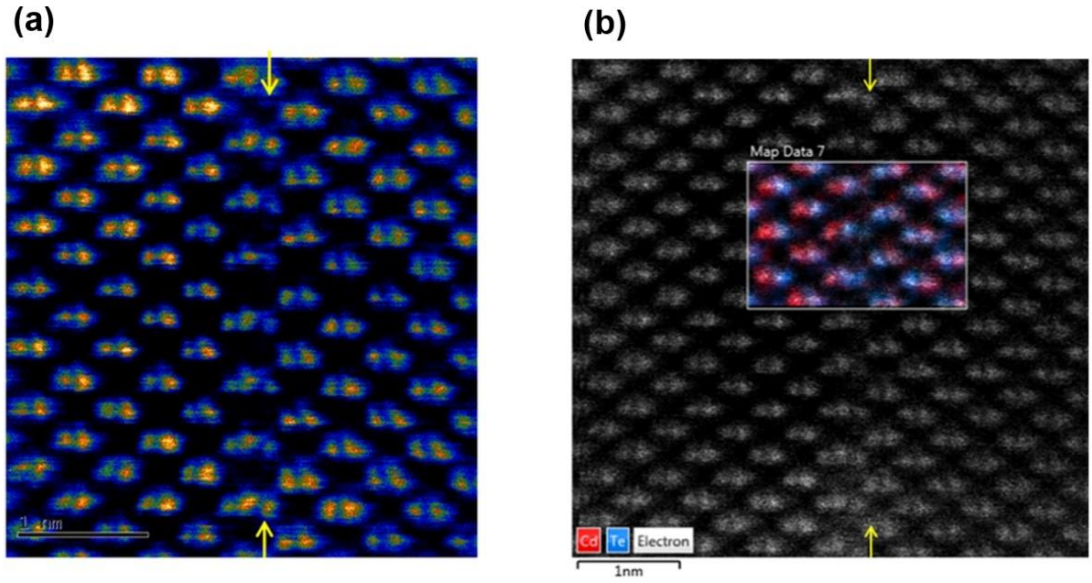

Figure S1. (a) Atomic-resolution HAADF image in temperature-coded colors of {001}B interface along <110> CdTe zone-axis. Position of the bonded interface is indicated by the arrows. (b) Atomic-resolution EDS map overlaid in color on the simultaneous HAADF image of the interface.

2. Energy dispersive X-ray spectroscopy (EDX) raw data

Figure S2 shows raw data of the atomic-resolution X-ray spectrum images used for the overlap in the main text Figure 1 (a). The bar-diagrams show horizontally summed X-ray counts. Tellurium monolayer presence can be seen from the middle Te peak in the bar diagram, and the horizontally running intensity in the 2D map. At the same time, Cd counts dip to the background X-ray levels at the position of tellurene layer.

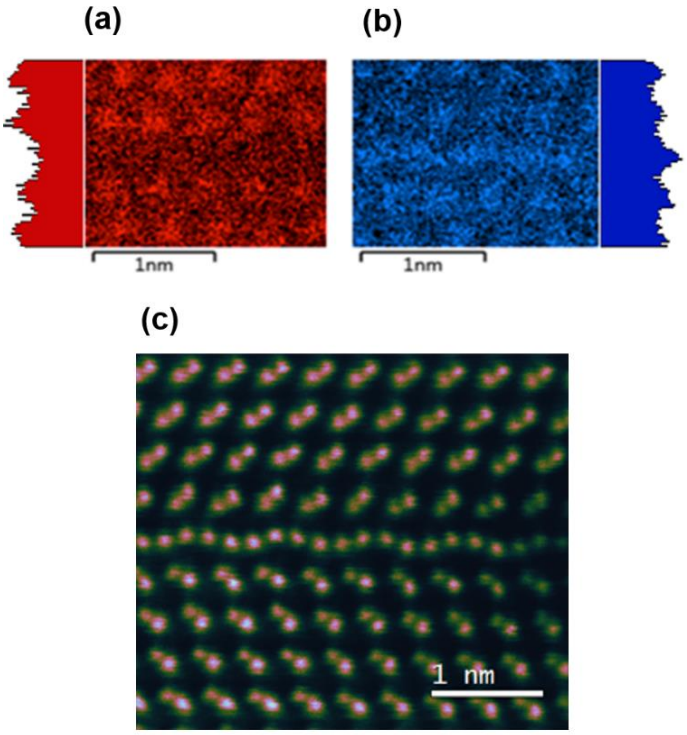

Figure S2. (a) Cd, (b) Te, color intensity represents a number of counts of $L\alpha_1$ emissions acquired over the scan time for a given electron probe position. Profiles show horizontally summed total counts. (c) Color-coded HAADF STEM image for a reference to the tellurene structure.

3. GW band structure and PBE without spin-orbit coupling

DFT-PBE band structure of tellurene interfacial structure without spin-orbit coupling (SOC) is plotted in Figure S3 (a), and compared to S3 (b) band energies from one-shot GW (G0W0) obtained by using the quasiparticle energies through Wannier interpolation within WANNIER90 program.[1-8] Wannier functions are projected using Cd -*s* and -*d*, and Te -*s* and -*p* orbitals. The band structure is calculated along the same special *k*-points as for PBE, along the *Γ*-*Y*-*S*-*X*-*Γ* direction, i.e., in-plane to tellurene surface. GW calculated band structure shown in Figure S3 (b)

is similar to the PBE such that tellurene is found to be metallic with linear band dispersions at *Y*, *S*, and *X*. Band crossings are also found at the *Y* and *X* *k*-points with GW.

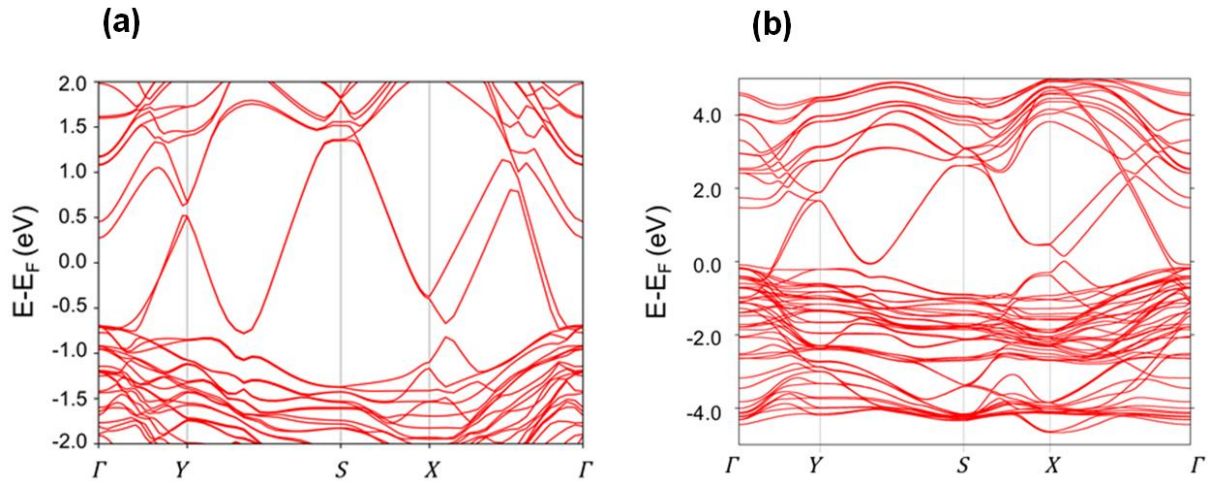

Figure S3. (a) DFT-PBE without spin-orbit coupling, and (b) GW calculated band structures of CdTe|tellurene|CdTe interface system.

4. Simulated EELS from GW calculations

The electron energy-loss spectra of bulk CdTe and tellurene system (CdTe|tellurene|CdTe) were calculated from the frequency-dependent dielectric function computed within the G_0W_0 approximation, as:

$$EELS(q,\omega) = -Im\frac{1}{\epsilon(q,\omega)}$$

The calculated EELS at q=0 Å^{-1} momentum transfer (optical approximation) of tellurene and bulk CdTe is shown in Figure S4. Bulk CdTe peak positions are in a general agreement with the measured bulk CdTe spectrum given in Figure 4 (d) in the main text, with relative intensities representative those of low-q transfer.[21] We also note that low-loss EELS of CdTe generally

shows very little dependence on the direction of momentum transfer indicating an isotropic dielectric function. The calculated tellurene EELS exhibits a single dominant peak (black curve) similarly to the experimental spectra. However, it is found at lower energy compared to the bulk CdTe volume plasmon, in contrast with the experiment. This discrepancy could arise due to the *q*-transfer dependent dispersion of the plasmonic excitation. In particular, the experimental EELS acquisition setup within STEM collects the electrons with *q*-transfer perpendicular to the imaging axis and ranging from q=0 to ~1.2 $Å^{-1}$, as defined by the beam convergence and the spectrometer collection angles.

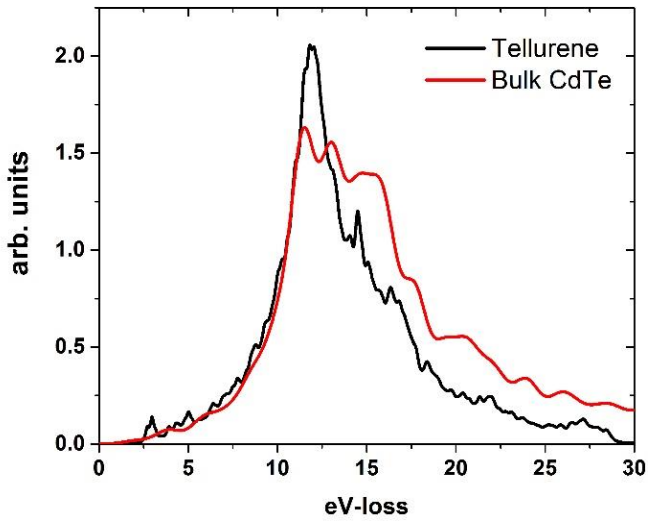

Figure S4. Calculated electron energy-loss spectra of tellurene (black) and bulk CdTe (red).

References:

1. Hedin, L., Physical Review 139, A796-A823, (1965).
2. Shishkin, M. & Kresse, G. Physical Review B 74, 035101, (2006).
3. Fuchs, F., Furthmüller, J., Bechstedt, F., Shishkin, M. & Kresse, G. Physical Review B 76, 115109, (2007).
4. Shishkin, M. & Kresse, G., Physical Review B 75, 235102, (2007).
5. Shishkin, M., Marsman, M. & Kresse, G., Physical Review Letters 99, 246403, (2007).
6. Marzari, N. & Vanderbilt, D., Physical review B 56, 12847 (1997).
7. Mostofi, A. A. et al., Computer physics communications 178, 685-699 (2008).
8. Souza, I., Marzari, N. & Vanderbilt, D., Physical Review B 65, 035109 (2001).